Europace Advance Access published April 21, 2010

Europace
doi:10.1093/europace/euq115

CLINICAL RESEARCH

12-lead surface electrocardiogram reconstruction from implanted device electrograms

G. Stuart Mendenhall* and Samir Saba

Department of Cardiac Electrophysiology, University of Pittsburgh Cardiovascular Institute, Pittsburgh, PA, USA

Received 28 January 2010; accepted after revision 25 March 2010

Aim Reconstruction of the surface electrocardiogram (EKG) from voltage recordings from implanted leads is not performed by current pacemakers or cardioverter-defibrillators. We investigated the feasibility and accuracy of reconstruction of a full 12-lead surface EKG from an implanted biventricular device.

Methods and results We applied three techniques for surface EKG reconstruction from multiple intracardiac (IC) vector recordings from implanted cardiac leads: single fixed dipole modelling via exact solution, exhaustive best-fit solution, and time-independent association using a transfer matrix. Recordings were performed at biventricular generator change in 10 patients. Overdetermined projection transformation resulted in high fidelity surface EKG reproduction for left-sided implanted devices (correlation coefficient 0.84 ± 0.13) with computationally lightweight reconstruction.

Conclusion After individual post-implantation correlation with the surface EKG, reconstruction using a time-independent transfer matrix accurately reproduces the surface EKG, is free from gating requirements, and retains validity during aberrant depolarization. These findings have significant implications for further study relating IC electrogram to surface tracings. The techniques may be used for real-time or remote monitoring and diagnosis of rhythm disturbances, cardiac ischaemia, and lead integrity and stability.

Keywords Electrocardiography • Pacemakers • Arrhythmia • Ischaemia • Computers

Introduction

The process of reconstruction of the overall depolarization pattern of the heart via recording of a subset of electrical potential difference vectors is generally classified as the 'inverse problem'. The 'forward problem' is the reverse, that is, the accurate reconstruction of an electrocardiogram (EKG) from knowledge of the spatio-temporal pattern of cardiac depolarization.

Single fixed dipole (SFD) representation of cardiac electrical forces models the summed electrical activity of the heart as a charge separation (electrical dipole) at the centre of the chest cavity. This single dipole can be projected onto various recording vectors and is widely taught to clinicians as a straightforward reduction of the electrical forces that give rise to the EKG. The magnitude and direction of the heart dipole changes with time, but the projected lead vectors' orientation to the centre of the dipole remains fixed. Prior studies have demonstrated variations of SFD modelling techniques for the correlation of EKG and body surface potential mapping,[1] straightforward interpolation of missing surface EKG leads,[2,3] and inverse problem solutions from measured body surface mapping potentials.[4–7]

Current implanted devices do not attempt reconstruction of surface electrocardiography or give depolarization waveform information to physicians for clinical interpretation. Given the extensive training and expertise that physicians invest in learning to recognize and interpret patterns in the standard 12-lead EKG recording, reconstruction of an accurate surface tracing representation from an implanted device may allow rapid diagnosis without external recording. Advantages of this system include low noise artefact from the fixed internal recording sources and the ability to obtain diagnostic tracings remotely from the implanted device. This may occur over telephone or internet networks upon symptom-driven patient activation, continuously, or upon device-detected changes in reconstructed EKG (rEKG) morphology.

In this article, we demonstrate the feasibility of reconstruction of a full surface 12-lead EKG from a series of intracardiac (IC) recordings from an implanted defibrillator with voltage leads in an arbitrary location through a transfer matrix relating IC to surface

* Corresponding author. Tel: +1 412 647 3429; fax: +1 412 647 0481, Email: gsmenden@post.harvard.edu

potentials in a time-independent fashion. The resultant reconstruction is highly correlated with the directly recorded surface EKG at the time of device implantation and retains validity during baseline and aberrant or ectopic cardiac depolarization.

Methods

All enrolled patients were undergoing generator change of an implanted biventricular cardioverter-defibrillator (ICD). Recordings were performed at the University of Pittsburgh Medical Center from June 2007 to June 2009. The UPMC institutional review board approved the study protocol and each patient gave written informed consent.

After detachment of the existing device generator, high impedance recording electrodes were connected directly to the four ventricular lead positions (proximal coil, distal coil, right ventricular electrode, left ventricular electrode) and the atrial lead. The recorded difference potentials include all or a subset of Can-RV, Can-RA, RA-RV, Can-Distal, Can-LV, Can-Prox, and RA-LV. An electrode connected to the tissue area at the site of the explanted device was used as a surrogate for the device 'can'.

All difference potentials were directly measured using the Prucka CardioLab EP system (GE Healthcare, Waukesha, WI, USA). Simultaneous measurement of all two-lead voltage tracings was obtained along with standard surface 12-lead EKG configuration (all algorithms) and modified-Frank vectorcardiogram (VCG)[8] (Algorithms 1a and 1b). Intracardiac tracings had hardware high-pass and low-pass filters set at 0.5 and 500 Hz, respectively, and EKG and vectorcardiographic tracings had recorded filtration boundaries of 0.5 and 500 Hz with a 60 Hz notch filter. The frequency of all data digital sampling was 977 Hz and stored as floating point value with 12-bit resolution. Hardware analogue-to-digital converter gain was adjusted to maximize signal to reduce loss of resolution with discrete quantization. If any saturation or clipping of recorded signal was observed, gain was reduced. Maximum signal gain used in this study was 5000. Given the method of reconstruction, results should be largely independent of the scaling or gain of the recorded electrogram, which would only alter the value of a row of the transfer matrix.

No spatial localization of implanted lead vectors by radiography was attempted or required during this study. All analysis was performed with MATLAB (The Mathworks, Inc., Natick, MA, USA) and C routines using code written by the authors and processed on a Intel Xeon server (IBM Corporation, Armonk, NY, USA) running the open source GNU/Linux v2.6 operating system.

Correlation methods

A general flowchart of both reconstruction algorithms is shown in *Figure 1*.

Algorithm 1a. *Single stationary dipole reconstruction (exact solution)*

Signal averaging was performed via a variant of moving window time-domain averaging. In this method of signal averaging, a manually selected reference QRST segment was obtained from a simultaneously recorded intracardiac set of difference potentials (IKG) and surface EKG during a period of baseline cardiac activity. Identification of subsequent cardiac cycles was made through comparison of the voltage tracing at every time point offset. For each point, the calculation of the R^2 sum of squares deviation from the reference segment for all corresponding leads was obtained, and time offsets that gave local minima that also fell under a threshold of 0.05 mV R^2 deviation were selected for signal averaging. This threshold was empirically determined and resulted in the inclusion of ~90% of measured QRS complexes while excluding any premature ventricular contractions, aberrantly conducted impulses, or beats with noise artefact. Post-recording filtration was performed using a finite impulse response (FIR) bandpass filter between 0.5 and 100 Hz.

Single dipole solutions were obtained by correlating three points of the corresponding signal-averaged IKG/EKG: maximal surface potential peak deflection in the VCG complex (maximum distance from isoelectric T–P origin), and two other points +30 ms and −30 ms before and after the maximum deflection. The resultant vector of each IC recording lead was noted and assumed to be fixed throughout the cardiac cycle and between recordings. The three recording points of the signal-averaged EKG, paired with the IC recordings, allow an exactly determined series of equations.

The relation at peak QRS deflection was established using matrix transformation ϕ:

$$E * \phi = S,$$

where E is a directly recorded time series of n simultaneous IC vectors, ϕ is an $n \times n$ matrix, and S is a simultaneous series of n surface recordings, of which three are linearly independent. Taking n time points at peak deflections of recorded E,

$$\phi = E^{-1} * S$$

providing that E is invertible. Reconstruction then is performed at all points using ϕ, which is held to be time-invariant.

Algorithm 1b. *Empiric fit single stationary dipole (exhaustive best-fit solution)*

Using simultaneous Frank VCG and IC recordings, signal averaging of the PQRST cardiac cycle was performed using the residual (R^2) minimization technique described above, in a computational 'brute force' technique. The averaged VCG was reprojected onto all possible vectors in a spherical co-ordinate system with 0.5° resolution. After bounded scaling using residual error minimization, the best-fit projection vector was found for each IC lead in relation to the VCG, and again for each surface lead in the 12-lead EKG in relation to the VCG. The VCG was reconstructed from the IC leads and reprojected to form a 12-lead EKG in a time-invariant fashion. Overall correlation coefficients for each patient were recorded.

Algorithm 2. *Correlation of overdetermined IC projections*

Modelling each of n simultaneous IC recording difference potentials recorded (E_n) to the entire 12-lead recording (V), we obtain

$$E * X = V.$$

The ($n \times 12$) transfer matrix X is used for subsequent reconstruction. X is obtained by minimization of the norm of the residual error z:

$$|z| = |V - E * X|$$

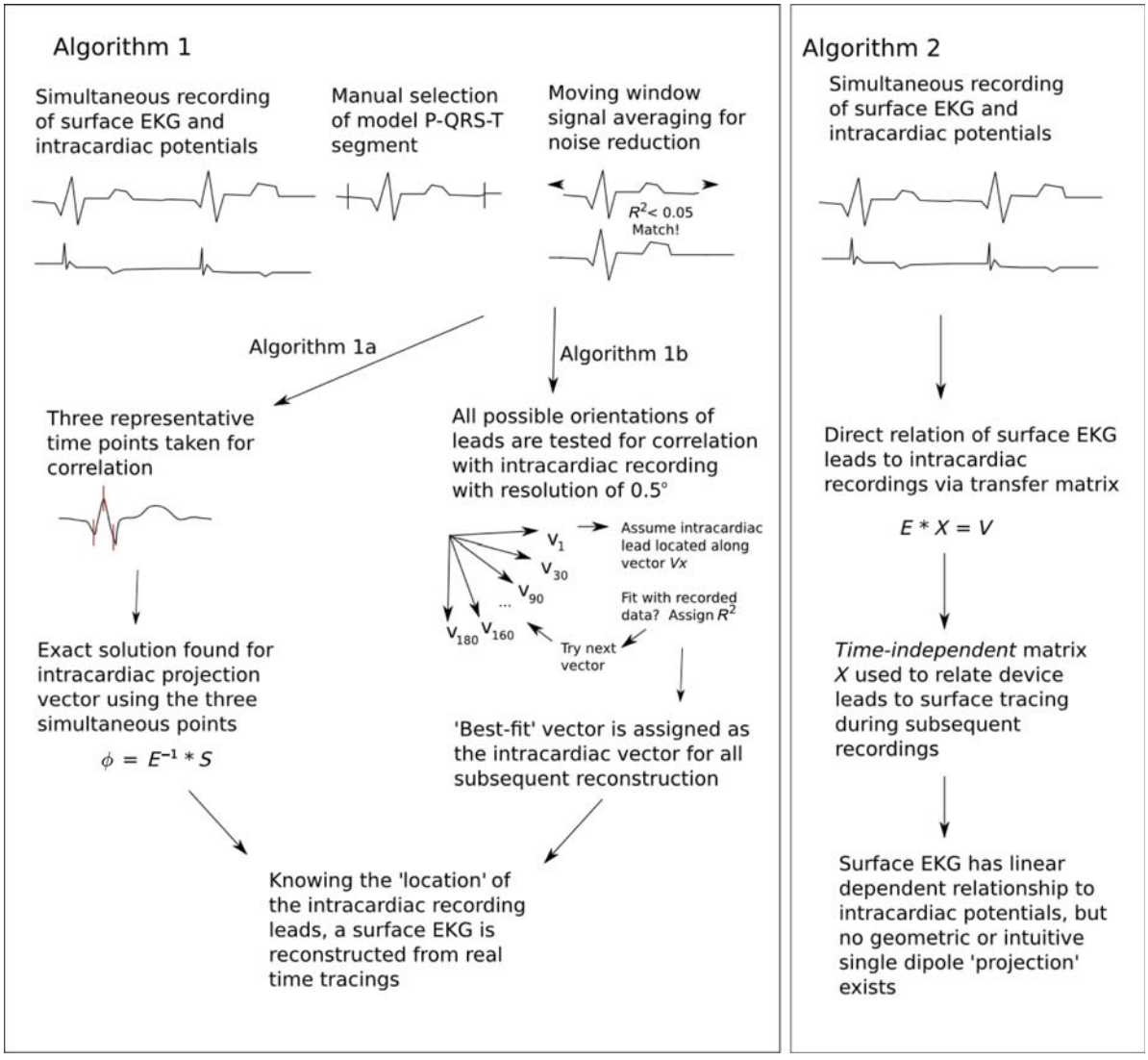

Figure 1 Methods of reconstruction.

for the correlation cycle. This solution was obtained via an algorithm adapted from Brannigan *et al.*,[9] and direct computation via QR factorization. In all patients, these methods produced identical solutions, and in this report, QR factorization is used via Householder transformation, in an algorithm adapted from standard techniques. Any matrices approaching singularity or underdetermined sets were assigned the null matrix and aborted the algorithm.

In Algorithm 2, correlation was performed over a 10 s simultaneous IKG–EKG recording period. Both EKG and IKG were filtered at 0.5 Hz high-pass filtration (HPF) and 100 Hz low-pass filtration (LPF) unless otherwise noted. The resulting transfer matrix *X* is time-independent and the 10 s recording period is arbitrary, as this algorithm does not require gating of QRS deflections nor any signal averaging. Reconstruction was then performed over a 4 s period, which was a minimum of 30 seconds after the correlation. Reconstruction used only IKG recordings and the transfer matrix and was compared with the simultaneous directly recorded surface EKG.

Statistical analysis

Accuracy of reconstruction was quantified by the calculation of Pearson's correlation coefficient between corresponding directly recorded EKG leads and rEKG leads at simultaneous data points. This was done for all correlated time points.

Results

Patient characteristics and recorded leads obtained are shown in *Table 1*. The mean age of patients was 69.5 $\pm$ 12.6 years. Nine of 10 patients had cardiomyopathy with reduced cardiac ejection fraction. One patient had a previously placed right-sided device due to occlusion in the left subclavian vein. All three methods of correlation and reconstruction were applied to all patients.

Table 1 Baseline patient characteristics

Pt no.	Age	Sex	Rhythm	QRS morphology	EF (%)	Pocket location	No. of IC leads	Leads	Notes
1	84	M	NSR (PVCs)	RBBB	20–25	L	8	1–8	NICM
2	58	M	AF	BiV paced	15–20	L	5	1–5	ICM s/p CABG
3	75	M	NSR	LBBB	35–40	L	5	1–5	ICM, severe PVD
4	60	M	NSR (PVCs)	LBBB	25–30	L	5	1–5	ICM, PAF
5	53	M	AF	Incomplete RBBB	25	L	6	1–6	ICM, Chronic AF
6	62	M	NSR	Narrow QRS Septal infarct	20–25	L	7	1–7	ICM, PAF
7	87	M	NSR	Narrow QRS Septal infarct	20	L	4	1–4	ICM, bioprosthetic MV
8	81	F	NSR	RV paced	50–55	L	5	2–6	NICM, hx VT (secondary prevention)
9	77	M	NSR (PVCs)	LBBB	20–25	R	8	1–8	NICM, infected system, recordings prior to removal
10	58	M	AF	LBBB	35	L	7	1–7	ICM

AF, atrial fibrillation; BiV, biventricular; CABG, coronary artery bypass grafting; IC, intracardiac; ICM, ischaemic cardiomyopathy; LBBB, left bundle branch block; MV, mitral valve; NICM, non-ischaemic cardiomyopathy; NSR, normal sinus rhythm; PAF, paroxysmal atrial fibrillation; PVC, premature ventricular contraction; PVD, peripheral vascular disease; RBBB, right bundle branch block; VT, ventricular tachycardia. Intracardiac lead numbering: 1. Can-RV; 2. Can-Distal; 3. Can-Proximal; 4. Can-RA; 5. Can-LV; 6. RA-LV; 7. RA-RV; 8. RV-LV.

A complete typical directly recorded intracardiac electrogram tracing (IKG) is shown in *Figure 2A*. In this tracing, the gain is set to a fixed value for all IC leads to demonstrate the relative amplitudes. The recorded leads that are outside and do not directly span the heart have lower amplitude as shown for comparison, but are amplified as described to maximize resolution for digital recording.

Algorithm performance

No sets of equations were underdetermined, and there were no singular or non-invertible solutions with correlation in all patients.

Single dipole modelling (Algorithms 1a and 1b)

Algorithms 1a and 1b gave similar results for correlation, with average Pearson correlation coefficients of 0.3–0.5 for lead reconstruction using single dipole reprojection. Average correlation (r) for Algorithm 1a in Patients 1–10 (all leads) was $0.49 \pm .32$ and for Algorithm 1b was $0.46 \pm .24$.

Overdetermined solution sets (Algorithm 2)

Reconstruction of surface EKG using overdetermined projection and transfer matrices (Algorithm 2) gives highly correlated tracing using implanted lead potentials, generally with overall correlation values of 0.9 or greater (*Table 2*).

Individual correlation coefficients for overdetermined projection transfer matrix for all patients are shown in *Table 2*, subdivided by EKG lead. A typical rEKG from an IC recording set is shown in *Figure 3* for Patients 1 (right bundle branch block) and 6 (normal QRS depolarization.).

Power and filtration

Intracardiac signals contained significant low-frequency component in the range of DC—20 Hz, dropping significantly and merging with the noise spectrum at higher frequencies greater than 50 Hz. Changes in morphology of the IKG filtered signal at various high-pass cut-off settings are shown in *Figure 2B–D*.

Limitation of high-frequency component with decreased LPF cut-offs (limitation of sharp deflections) could lead to a 'smoothing effect' and improved correlation. To investigate the effects of varying filter cut-offs, correlation at baseline was performed at various HPF and LPF settings. Limitation of high-frequency components (decreasing LPF) from 100 to 50 Hz improved overall correlation, but further reduction had minimal benefits. Correlation decreased sharply with increase in HPF past 3 Hz at baseline but did not drop with reduction to 0.5 Hz, also evident in the high-quality reconstructions in *Figure 3*. This suggests that the optimal filtration for reconstruction is similar to that of surface EKG recording, namely 0.5–50 Hz bandpass. Slight limitation of high-frequency component on the IKG may blunt near-field effects and improve reconstruction.

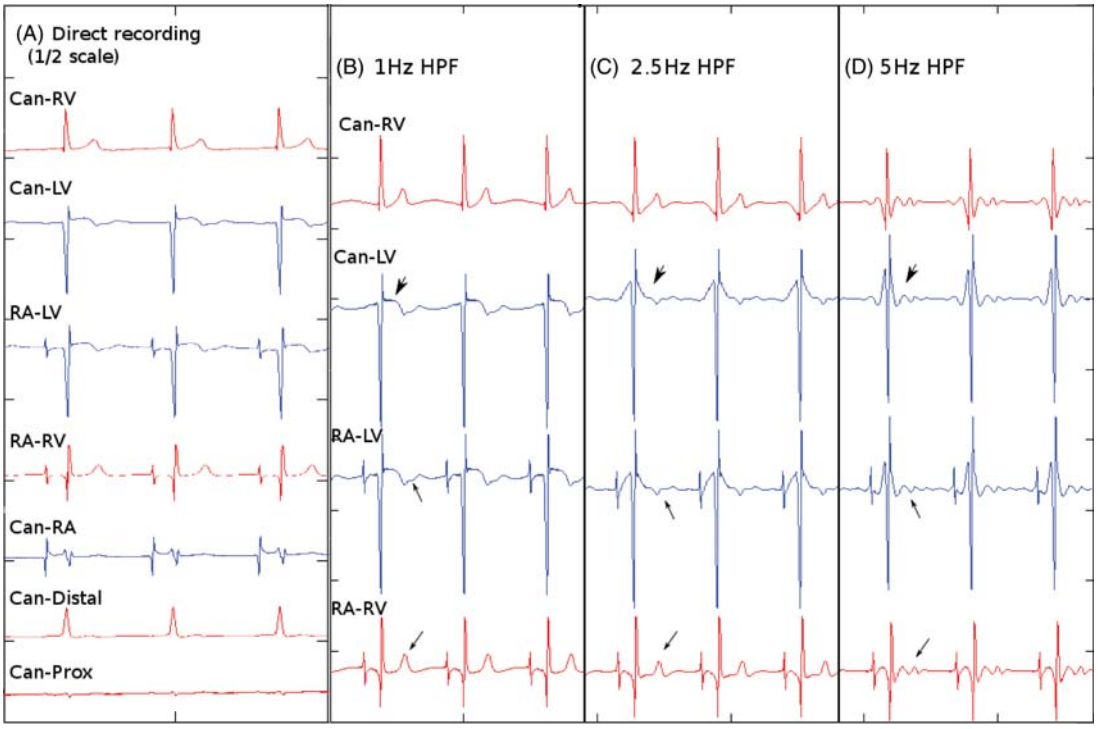

Figure 2 Intracardiac recordings and filtration effects. (*A*) Sample intracardiac recording set (IKG) from Patient 6. For all tracings, markers on the *x*-axis are every 2000 samples (~2 s.) The can-proximal coil recording has significantly lower amplitude than other IC tracings due to the distance of this recording vector from the heart. Tracing A has no digital filtration (hardware HPF = 0.5 Hz, LPF = 500 Hz). All leads are simultaneously recorded. Of note, figure A has vertical (amplitude) $\frac{1}{2}$ scale compared with tracings B–D. (*B–D*) Effect of electrogram filtration. Recording set with HPF set at 1 Hz (*B*), 2.5 Hz (*C*), and 5 Hz (*D*). Low-frequency components are progressively lost with alteration of the T-wave (small arrowheads) and loss of ST segment offset (large arrowheads) as the HPF cut-off is raised.

Table 2 Correlation coefficients for overdetermined projection (Algorithm 2)

Patient	1	2	3	4	5	6	7	8	9	10
I	0.94	0.67	0.94	0.82	0.73	0.86	0.69	0.97	0.44	0.85
II	0.98	0.77	0.61	0.79	0.78	0.97	0.87	0.93	0.11	0.9
III	0.94	0.8	0.94	0.8	0.64	0.91	0.91	0.95	0.1	0.88
AvR	0.99	0.72	0.88	0.82	0.76	0.94	0.83	0.88	0.14	0.91
AvL	0.82	0.8	0.96	0.81	0.58	0.85	0.92	0.96	0.11	0.88
AvF	0.97	0.79	0.82	0.8	0.6	0.95	0.89	0.95	0.11	0.89
V1	0.66	0.82	0.89	0.95	0.56	0.91	0.77	0.96	0.21	0.97
V2	0.9	0.84	0.46	0.98	0.8	0.9	0.91	0.97	0.14	0.98
V3	0.98	0.63	0.79	0.96	0.86	0.89	0.92	0.98	0.15	0.97
V4	0.99	0.57	0.78	0.91	0.85	0.87	0.96	0.98	0.14	0.94
V5	0.99	0.62	0.62	0.76	0.75	0.88	0.86	0.91	0.15	0.22
V6	0.99	0.63	0.8	0.74	0.7	0.9	0.81	0.72	0.28	0.9

Pacing artefact

Large amplitude pacing depolarization interfered with correlation independent of signal saturation of analogue-to-digital conversion (Patient 2 in *Table 2*), possibly due to further deviance from ideal single dipole and effects of differential capacitance. Manual removal of pacing artefact did not significantly change correlation values (not shown).

Lead subsets

Average correlation coefficients with Algorithm 2 using reduced lead subsets are shown in *Table 3*. In this table, reconstruction is

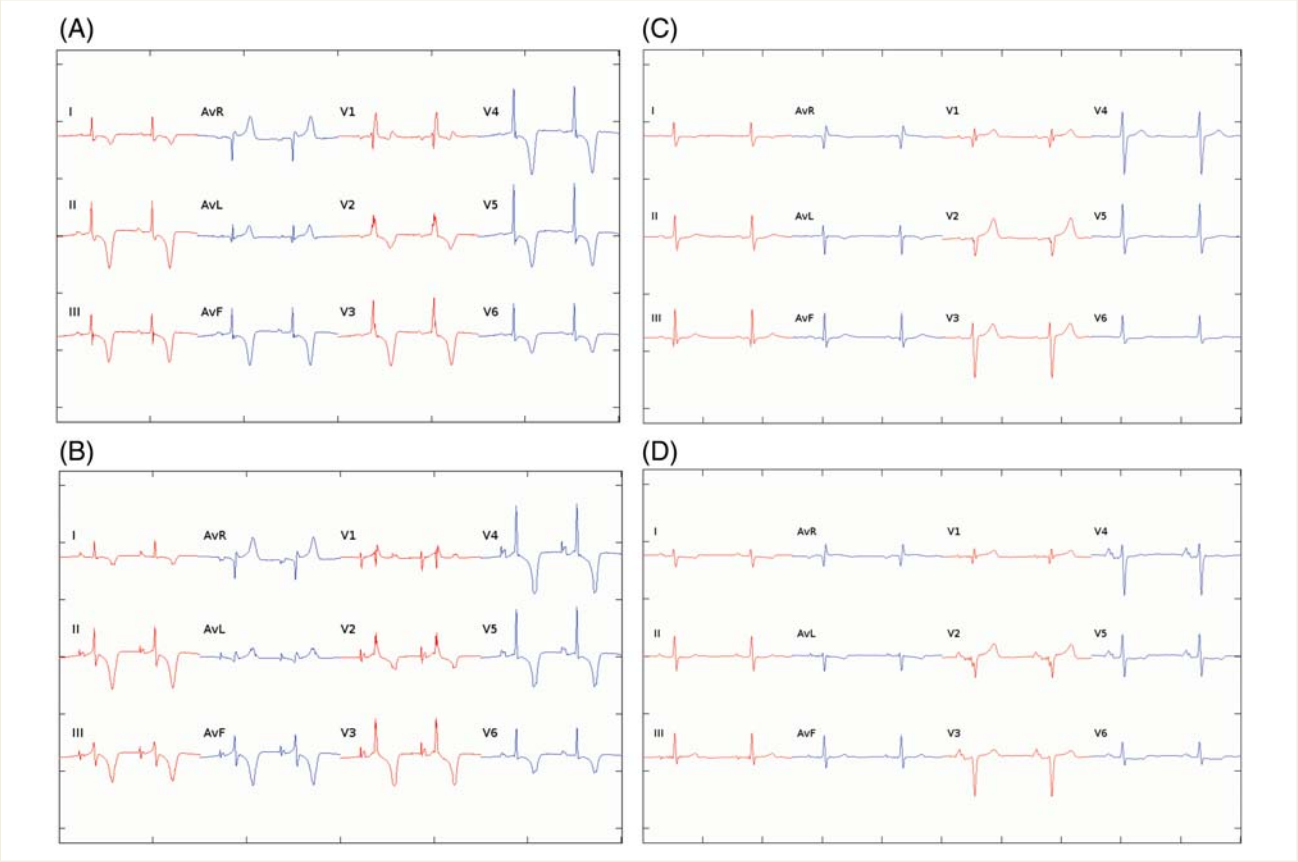

Figure 3 Directly recorded EKG and rEKGs. (*A*) Directly recorded EKG tracing of Patient 1. All leads are simultaneously recorded but displayed in standard sequential format. (*B*) rEKG from IC recording set of Patient 1. (*C*) Directly recorded EKG tracing of Patient 6. (*D*) Reconstructed (rEKG) of Patient 6.

Table 3 Reduced lead set correlation results

Number of leads	*n*	*R*	SD
8	1	0.92	–
7	3	0.90	0.03
6	4	0.85	0.14
5	8	0.78	0.19
4	10	0.75	0.18
3	10	0.72	0.17
2	10	0.62	0.18

Correlation coefficients resulting from Algorithm 2 using reduced number of IC leads. Reconstruction was performed using two-lead subset (Can-Distal and Can-Prox electrograms) on all patients. Additional leads were added to the algorithm and correlation was reassessed. Leads were added in order: Can-RA, Can-LV, RA-LV, and RA-RV. Any patient without sufficient directly recorded electrograms was used in the total. Patient 9 was not included in >4 lead reconstruction due to the right-sided device placement and co-linearity of IC vectors.

solely provided from a subset of the IKG leads, and the average correlation value for all 12-surface leads is shown. Increased numbers of leads improved correlation, with optimal reconstruction with 7+ leads. Under no observed cases did addition of recording leads reduce correlation.

Computational efficiency

Correlation took from 10 to 30 s on this server for each algorithm, although the interpreted language and software FIR filtration routines leave significant areas for optimization. Reconstruction of the surface EKG from IC recording vectors required only matrix multiplication operations that remain a lightweight calculation. Reconstruction may be performed using current implanted device CPU systems in real time (millisecond delay) once correlation has been established.

Discussion

Using implanted device data, simple single dipole reprojection (Algorithms 1a and 1b) does not give satisfactory results, with high R^2 value, low correlation value, and poor major deflection of QRS concordance between directly recorded and rEKG tracings. While conceptually attractive, SFD reconstruction is limited by the presence of heterogeneity in torso conduction properties and translation of the depolarization wavefront as it

traverses across the heart. The success of Algorithm 2 is accounted by lead theory, which models current flow instead of single projection of a static field along a line vector. Each recording vector is assigned a weight in the transfer matrix that represents its component of the resultant summation EKG.

Number of leads

Using overdetermined projection, obtaining IKG leads that span greater distances of cardiac depolarization or are highly concordant with the measured EKG vector are essential for accurate reconstruction. Placement of a right-sided device and concurrent loss of lead recordings representative of large areas of solid angle around the electrical generator source is associated with poor correlation, as evidenced by Patient 9 (*Tables 1* and *2*). Similar to right-sided device placement, limitation of the number and location of recording vectors reduces the fidelity of reconstruction.

Given the properties of Algorithm 2, additional redundancy of recording vectors should not reduce correlation due to the optimization of the transfer matrix. Any leads that are poorly correlated, noisy, or otherwise undesirable for reconstruction of a given lead would be proportionally devalued. An uncorrelated IC lead would result in a row of low values or zeros in matrix *X*, but should not significantly reduce overall correlation. To maximize reconstruction fidelity, future devices or lead systems may be designed to encompass as much solid angle around the heart as possible, yielding an extensive IKG for subsequent correlation.

Lower values of correlation were often associated with low-amplitude signals, particularly during low-amplitude recording across the precordium near R-wave transition points. Small deviations in major deflection (primarily R-wave vs. primarily S-wave) exhibit poor correlation, but may be visually accurate and have no effect on tracing interpretation.

Near-field effects

All IC reconstruction techniques are also complicated by near-field potential artefact and the discontinuities that develop from them. In SFD modelling, projection along an axis is not dependent on the distance from the recording sites to the source of depolarization. However, as the wavefront approaches the recording lead, high electrical potential is recorded largely independently of the wavefront propagation direction and assumptions in SFD modelling break down.

P-waves are often accentuated on rEKGs with an increased rapid deflection. This artefact is due to near-field prominence in the EKG (*Figure 2A*, Can-RA, RA-RV, RA-LV tracings), coupled with relative low amplitude of the far-field P-wave on direct measurement. This may be removed by gating of tracing and using separate correlation during segments of the PQRS cycle. However, any requirements for gating during reconstruction (time-/phase-dependent reconstruction) reduce the generalizability in various rhythms (SVT/VT), add complexity, and increase the need for extensive validation. In the current forum, Algorithm 2 does not have time-varying reconstruction requirements. Visualization of a reconstructed P-wave, regardless of where it falls in the PQRST cycle, may assist in the clinical interpretation of various rhythms such as SVT and VT discrimination. In this study, the three patients in atrial fibrillation had rEKGs with a baseline that appeared similar to surface recording of AF.

Cardiac motion

In the standard EKG, the leads are fixed to the body surface, while implanted cardiac leads that are fixed to the heart move in tandem with portions of the myocardium. Moreover, these may move in a different motion during aberrant conduction or ectopic beats, a motion that depends on electromechanical coupling and is unpredictable until direct measurement. In the absence of respiratory gating and time-dependent reconstruction, this artefact is unavoidable and inherent to the recorded lead locations. However, during baseline correlation, the excellent results obtained using Algorithm 2 indicate that this is not a limiting factor in achieving high-quality reconstruction.

Signal averaging and gating

If needed, minimization of residual from moving time-window techniques for identification of both gating and signal averaging allows both quantification of the QRS concordance to baseline recording in addition to cardiac phase detection. Of note, gating must be done after a full cardiac cycle is recorded, giving a slight delay in the reconstruction of approximately one cycle length.

Implementation of QRS gating during aberrant conduction or ectopic beats has clear benefits; a ventricular complex with morphology similar to the native QRS will be detected and aligned as best fit. For gating-dependent algorithms, numerous PVCs at the time of implantation could be simultaneously recorded and form a 'library' of aberrancy or ectopy that could be interpolated for accurate reconstruction.

SVT/VT discrimination

An immediate and direct application of these techniques is the use for rapid quantitative assessment of depolarization matches for tachycardia discrimination. The derived EKG match takes into account timing and morphology from all implanted leads, and a quantitative index of R^2 deviation at maximum coherence is readily available using moving window signal averaging.

This technique has particular advantages over current systems in implanted devices that use template matching from single ventricular electrograms, where an abnormal ventricular conduction pattern could project to a similar single electrogram pattern. With IC-derived rEKG, while a single IC lead may be similar during a different cardiac rhythm, the rEKG will be scored as a higher degree mismatch due to the incorporation of data from all electrodes. Secondly, the nature of the moving window temporal alignment algorithm ensures accurate gating if there is a morphology match anywhere in the cardiac cycle. There are no problems with gating off T-waves as with simple peak detection given multiple lead configuration and the possibility of searching all time points.

Ischaemia

The linear transformation used in overdetermined projection reconstruction methods keeps a fixed origin. Thus, the period of electrical neutrality, corresponding to the TP segment, will be well correlated due to the relative length of this period in relation

to the QRS segment. This has immediate applicability for the detection of resting currents or ST segment deviation. We have previously shown[10] that IC ST deviation with ischaemia induced in an animal is reliably detected on direct IC recordings. Thus, if appropriate filtration is maintained, ST elevation, modelled as a DC offset of s millivolt on IC lead E_y, is obtained by

$$(E_y + s) * X = E_y * X + s * X$$

given the properties of the linear operator X. If an IC lead set has a single raised IC voltage offset, this will map to surface leads in all transformations X providing that X has no rows of zeros.

A high fraction of pacing is expected with biventricular devices, but intermittent recording of native QRST complexes, if available, would provide ST deviation information. Since this reconstruction depends only on the relationship between the surface and IC leads, the validity of ST deviation should remain despite any repolarization alteration due to T-wave 'memory' effects.

Filtration requirements

Most currently manufactured devices use hardware filtration prior to analogue-to-digital conversion to eliminate baseline wander due to low-frequency electric fields and to reduce T-wave oversensing. This is often in the range of 2 Hz HPF. As demonstrated in *Figure 2B–D*, significant information is maintained in this frequency range, and loss of this low-frequency signal can cause marked morphology changes to the observer in slowly time-varying components, such as ST segments or the T-wave or repolarization pattern. The HPF cut-off could be lower than a standard surface EKG given the relative insulation from slowly varying external fields and absence of requirement of extremely high reliability of QRS detection as standard ICD and pacemaker algorithms dictate.

Limitations, implications, and future directions

Limitations of this study include the low numbers of patient enrolment due to the need to directly access the implanted leads, the single visit period of reconstruction, and lack of changes in study patient's EKG over different clinical conditions or long time periods.

Once established and validated, there are significant applications for remote diagnosis on a symptom activated or continuous basis. Coupled with currently available remote transmission, physician over-read may provide appropriate patient triage and treatment if specificity and sensitivity are maintained. With routine rEKG snapshots stored or transmitted by the implanted device, facilitation of our understanding of any cardiac electrical alteration or events preceding ischaemia or dysrhythmias will be obtained from retrospective analysis of patients who present with capable devices. This is a promising tool for future research.

Conclusions

We have demonstrated a method for highly accurate reconstruction of the surface EKG from an implanted device after a single initial correlation. As the robustness of these algorithms becomes empirically established, these findings have significant implication for remote monitoring and diagnosis. In its current form, this device algorithm allows accurate reconstruction of the baseline surface EKG. Coupled with gating and deviation assessment, differences in this reconstructed tracing would detect aberrant conduction patterns or ectopic depolarization with high sensitivity. If a deviation is confined to a single lead, this could suggest lead problems such as dislodgement or migration. Monitoring of ST segment deviation in the reconstruction is, in our theoretical calculations, expected to have high correlation with injury current seen on direct recording of the EKG. Hardware filtration prevents this technique from being used without device modification for current implanted ICD systems. Further studies will evaluate stability of these reconstructions over long periods of time and perform empiric validation under various clinical conditions.

Conflict of interest: None declared.

Funding

This work was supported by University of Pittsburgh Academic Seed Funds.

References

1. Gabor D, Nelson CV. Determination of the resultant dipole of the heart from measurements on the body surface. *J Appl Phys* 1954;**25**:413–6.
2. Dower GE, Machado HB, Osborne JA. On deriving the electrocardiogram from vectorcardiographic leads. *Clin Cardiol* 1980;**3**:87–95.
3. Uijen GJH, van Oosterom A, van Dam RT. The relationship between the 12-lead standard ECG and the XYZ vector leads. In Proceedings of 14th International Congress on Electrocardiography. Berlin: Academy of Sciences of the DDR 1998.
4. Horan LG, Flowers NC. Recovery of the moving dipole from surface potential recordings. *Am Heart J* 1971;**82**:207–14.
5. Barr RC, Ramsey M, Spach MS. Relating epicardial to body surface potential distributions by means of transfer coefficients based on geometry measurements. *IEEE Trans Biomed Eng* 1977;**24**:1–11.
6. Barr RC, Spach MS. Inverse calculation of QRS-T epicardial potentials from body surface potential distributions for normal and ectopic beats in the intact dog. *Circ Res* 1978;**42**:661–75.
7. Huiskamp G, van Oosterom A. The depolarization sequence of the human heart surface computed from measured body surface potentials. *IEEE Trans Biomed Eng* 1998;**35**:1047–58.
8. Frank E. An accurate, clinically practical system for spatial vectorcardiography. *Circulation* 1956;**13**:737–49.
9. Brannigan M. The strict Chebyshev solution of overdetermined systems of linear equations with rank deficient matrix. *Numerische Mathematik* 1982;**40**:307–18.
10. Williams JL, Mendenhall GS, Saba S. Effect of ischemia on implantable defibrillator intracardiac shock electrograms. *J Cardiovasc Electrophysiol* 2007;**19**:275–81.